

A refined nonlinear least-squares method for the rational approximation problem

Michael S. Ackermann* Linus Balicki*
 Serkan Gugercin† Steffen W. R. Werner§

**Department of Mathematics, Virginia Tech, Blacksburg, VA 24061, USA.*

Email: amike98@vt.edu, ORCID: [0000-0003-3581-6299](https://orcid.org/0000-0003-3581-6299)

† *Department of Mathematics, Virginia Tech, Blacksburg, VA 24061, USA.*

Email: balicki@vt.edu, ORCID: [0000-0002-8901-2889](https://orcid.org/0000-0002-8901-2889)

‡*Department of Mathematics and Division of Computational Modeling and Data Analytics, Academy of Data Science, Virginia Tech, Blacksburg, VA 24061, USA.*

Email: gugercin@vt.edu, ORCID: [0000-0003-4564-5999](https://orcid.org/0000-0003-4564-5999)

§*Department of Mathematics, Division of Computational Modeling and Data Analytics, and National Security Institute, Virginia Tech, Blacksburg, VA 24061, USA.*

Email: steffen.werner@vt.edu, ORCID: [0000-0003-1667-4862](https://orcid.org/0000-0003-1667-4862)

Abstract: The adaptive Antoulas-Anderson (AAA) algorithm for rational approximation is a widely used method for the efficient construction of highly accurate rational approximations to given data. While AAA can often produce rational approximations accurate to any prescribed tolerance, these approximations may have degrees larger than what is actually required to meet the given tolerance. In this work, we consider the adaptive construction of interpolating rational approximations while aiming for the smallest feasible degree to satisfy a given error tolerance. To this end, we introduce refinement approaches to the linear least-squares step of the classical AAA algorithm that aim to minimize the true nonlinear least-squares error with respect to the given data. Furthermore, we theoretically analyze the derived approaches in terms of the corresponding gradients from the resulting minimization problems and use these insights to propose a new greedy framework that ensures monotonic error convergence. Numerical examples from function approximation and model order reduction verify the effectiveness of the proposed algorithm to construct accurate rational approximations of small degrees.

Keywords: data-driven modeling, reduced-order modeling, rational functions, barycentric forms, nonlinear optimization

Mathematics subject classification: 41A20, 65D15, 93B15, 93C05, 93C80

Novelty statement: We develop a new greedy-type adaptive approximation method for the construction of rational approximations from given data. The proposed method selects in every step a suitable interpolation point to minimize an error measure and efficiently solves a nonlinear least-squares problem on the rest of the data. We provide a theoretical analysis of the minimization approaches in terms of their gradients.

1 Introduction

Approximating complex functions by rational functions is an important task in the computational sciences. A recent popular approach for this purpose is the adaptive Antoulas-Anderson (AAA) algorithm [24], which had wide ranging success in many fields due to its ability to achieve highly accurate approximations quickly; see [25] for a survey of the method. In certain applications, it is desired to construct highly accurate rational functions that have a low degree. One of these applications is model order reduction in the frequency domain [2, 4, 7]. Here, the input-to-output behavior of a dynamical system can be described via a rational function, the so-called transfer function. The degree of that rational function is also the order of the corresponding dynamical system. The task in model order reduction is then to find a rational approximation to the transfer function that is accurate in regions of interest while having the smallest possible degree to ensure fast evaluations.

Data-driven reduced-order modeling has become common practice. In this paper, we focus on data-driven reduced-order modeling grounded in rational approximation theory. For an incomplete list of such methods, see, e.g., [3, 4, 8, 9, 12–14, 16, 22] and the references therein. Many of these works satisfy optimality conditions, provide error bounds, or offer specialized nonlinear optimization techniques, all with the goal of providing the most accuracy with a low degree rational function. Our focus in this paper is on the AAA algorithm and our proposed method, NL-AAA, which we demonstrate can provide reliably better accuracy at a lower order than AAA.

While the AAA method is an adaptive tool that allows the construction of rational approximations to a certain error tolerance, in some cases the error convergence can be unpredictable which might lead to an unnecessarily high degree rational approximant. Consider as example two functions: the absolute value $|x|$ and the rectified linear unit (ReLU) with $\text{relu}(x) = \max(x, 0)$, both in the interval $[-1, 1]$. We use 501 linearly equidistant evaluations of each function to compute rational approximations. The results of this experiment are shown in [Figure 1](#) in terms of the normalized ℓ_2 error vs the degree of the rational functions; see [Section 5.1](#) for the definition of the error measure. While AAA performs very well on the absolute value, it barely converges for the ReLU function. In contrast, we propose in this work the NL-AAA algorithm, which performs similarly well compared to AAA for the absolute value and completely outperforms AAA for ReLU. Thereby, we showcase that there are more suitable methods for applications in which low-degree rational functions are needed. Additionally, we note that in contrast to the classical AAA, the error behavior of the proposed NL-AAA method is monotonic.

In this work, the task at hand is the construction of rational approximations $r(z)$ for given data sets of the form $\{(z_i, H(z_i))\}_{i=1}^M$, where $z_i \in \mathbb{C}$ are the evaluation points and $H(z_i)$ the corresponding function evaluations. Thereby, we aim to reach a prescribed level of accuracy with $r(z)$ with respect to the given data, while keeping the degree of $r(z)$ as low as possible. To this end, we propose modifications to the classical AAA algorithm by solving the true rational least-squares problem in every step using the Sanathanan-Koerner iteration [27] and Whitfield's iteration [28]. By deriving the gradients of these different methods in the Wirtinger calculus, we can show that our proposed NL-AAA algorithm cheaply solves the rational least-squares problem of interest in every step rather than the approximation done by AAA. Furthermore, our analysis allows us to characterize the performance of the classical AAA and ensures that our proposed method converges monotonically with increasing degree of the approximation.

The remainder of this work is organized as follows. In [Section 2](#), we review the model

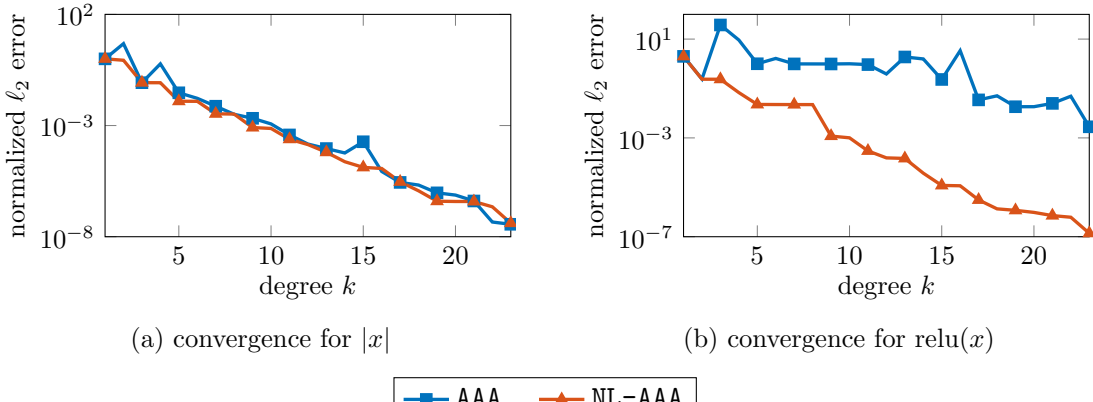


Figure 1: Convergence behavior of the classical AAA algorithm and the newly proposed NL-AAA method on two test functions: In both cases, NL-AAA decreases the error monotonically. While for the absolute value, both methods show a very similar performance, for the ReLU function, the proposed method obtains smaller approximation errors significantly faster than the classical AAA approach.

order reduction problem and the fundamentals of AAA, reformulated for the purpose of this paper. In [Section 3](#), we review two iterative methods for solving the rational least-squares problem, namely the Sanathanan-Koerner iteration and Whitfield's iteration, and formulate these for the barycentric form. We then present our proposed algorithm, NL-AAA, in [Section 4](#) and analyze the different refinement approaches for solving the rational least-squares problem in terms of their gradients. Numerical experiments presented in [Section 5](#) are used to compare the classical AAA approach and the proposed NL-AAA method on function approximation as well as model order reduction examples. The paper is concluded in [Section 6](#).

2 Mathematical preliminaries

In this section, we give a brief introduction to the model order reduction problem and its connection to rational approximation. After introducing the proper interpolatory barycentric form, we review the classical AAA algorithm for rational approximation from [\[24\]](#) as well as the idea of the Levy approximation [\[20\]](#) to the rational nonlinear least-squares problem, which is an essential component in AAA.

2.1 Model order reduction via rational approximation

Linear time-invariant dynamical systems can be written as systems of differential and algebraic equations of the form

$$\mathbf{E}\dot{\mathbf{x}}(t) = \mathbf{A}\mathbf{x}(t) + \mathbf{b}u(t) \quad (1a)$$

$$y(t) = \mathbf{c}^T \mathbf{x}(t), \quad (1b)$$

where $\mathbf{A}, \mathbf{E} \in \mathbb{C}^{N \times N}$ and $\mathbf{b}, \mathbf{c} \in \mathbb{C}^N$ are the system matrices, $\mathbf{x}: \mathbb{R} \rightarrow \mathbb{C}^N$ is the internal system state, $u(t): \mathbb{R} \rightarrow \mathbb{C}$ is the input to the system, and $y(t): \mathbb{R} \rightarrow \mathbb{C}$ is the external output of the system. We assume that the matrix pencil $\lambda\mathbf{E} - \mathbf{A}$ has at most one infinite eigenvalue. Using the Laplace transform, the system [\(1\)](#) can equivalently be described in

the frequency (Laplace) domain via its corresponding transfer function

$$H(z) = \mathbf{c}^T(z\mathbf{E} - \mathbf{A})^{-1}\mathbf{b}. \quad (2)$$

The function $H : \mathbb{C} \rightarrow \mathbb{C}$ is a degree- N proper rational function, which yields a direct relation between the system input and output.

The main computational costs for evaluating (1) in applications stems from the number of differential equations and the corresponding dimension of the state vector N . In many applications, which demand for high modeling accuracy, the dimension N is large ($N \in \mathcal{O}(10^6)$). Consequently, the evaluation of (1) is associated with high computational costs in terms of computation time and memory demands. To mitigate these issues, model order reduction aims to construct cheap-to-evaluate surrogate models of the same form

$$\widehat{\mathbf{E}}\dot{\widehat{\mathbf{x}}}(t) = \widehat{\mathbf{A}}\widehat{\mathbf{x}}(t) + \widehat{\mathbf{b}}u(t) \quad (3a)$$

$$\widehat{y}(t) = \widehat{\mathbf{c}}^T\widehat{\mathbf{x}}(t), \quad (3b)$$

where $\widehat{\mathbf{E}}, \widehat{\mathbf{A}} \in \mathbb{C}^{k \times k}$, $\widehat{\mathbf{b}}, \widehat{\mathbf{c}} \in \mathbb{C}^k$, and with the internal dimension $k \ll N$. The corresponding transfer function is then given as

$$r(z) = \widehat{\mathbf{c}}^T(z\widehat{\mathbf{E}} - \widehat{\mathbf{A}})^{-1}\widehat{\mathbf{b}}. \quad (4)$$

These surrogate models are aimed to accurately approximate the original system's input-to-output behavior. In the frequency domain, this approximation problem is equivalent to finding a rational function of degree k that approximates the transfer function of the original model (2); see, for example, [2, 6].

Explicit full-order models like (1) are not always readily accessible; for example, in the cases of complex dynamical processes, which cannot easily be modeled via first-principle theories. However, in these cases, typically input-output data is available instead. In the frequency domain, such data corresponds to evaluations of the transfer function (2) in given frequency points $\{z_i\}_{i=1}^M$ such that the given data takes the form of tuples $\{z_i, H(z_i)\}_{i=1}^M$. In this setting of data-driven reduced-order modeling, the goal is to approximate the given data in a suitable way by constructing a degree- k rational function [4, 7]. The approaches described in this work can be applied in both scenarios, i.e., for model order reduction and data-driven modeling.

2.2 The interpolatory barycentric form

A rational function $r : \mathbb{C} \rightarrow \mathbb{C}$ is said to have the degree $k - 1$ if it can be written as the ratio of degree- $(k - 1)$ polynomials. If the rational function r has no poles in the k complex points $\lambda_1, \dots, \lambda_k \in \mathbb{C}$, then it can be expressed via the interpolatory barycentric form

$$r(z) = \frac{n(z)}{d(z)} = \frac{\sum_{j=1}^k w_j \frac{h_j}{z - \lambda_j}}{\sum_{j=1}^k w_j \frac{1}{z - \lambda_j}}. \quad (5)$$

In (5), the points $\lambda_1, \dots, \lambda_k \in \mathbb{C}$ are called the barycentric support points, $h_1, \dots, h_k \in \mathbb{C}$ are function values, and $w_1, \dots, w_k \in \mathbb{C}$ are called the barycentric weights. For any nonzero barycentric weight w_j , the representation (5) has a removable singularity in the corresponding expansion point λ_j in which it can be expanded to take the corresponding

function value h_j . Thus, the continuous extension of the rational function r satisfies the interpolation conditions $r(z_j) = h_j$, for $j = 1, \dots, k$; see [3, 10].

For fixed support points and functions values, to employ (5) in the context of approximating functions or data, the barycentric weights can be seen as free parameters. These weights can be used to enforce additional interpolation conditions or to minimize other error measures with respect to the approximated function or the given data. We note that the weights w_j in (5) are generally non-unique since scaling each weight by the same constant does not change the rational function r . This non-uniqueness is typically resolved by either requiring that the vector of weights has length 1 in some suitable norm or by setting one the weights constant, e.g., $w_1 = 1$.

In the context of model order reduction, the matrix representation of rational functions in the form (4) is needed for time domain evaluations of the corresponding system. To recover the system matrices from the parameters of the barycentric form, define

$$\hat{\mathbf{E}} = \begin{bmatrix} 1 & -1 & & \\ \vdots & & \ddots & \\ 1 & & & -1 \\ 0 & 0 & \dots & 0 \end{bmatrix}, \quad \hat{\mathbf{A}} = \begin{bmatrix} \lambda_1 & -\lambda_2 & & \\ \vdots & & \ddots & \\ \lambda_1 & & & -\lambda_k \\ -h_1 w_1 & -h_2 w_2 & \dots & -h_k w_k \end{bmatrix}, \quad (6a)$$

$$\hat{\mathbf{b}} = [0 \ \dots \ 0 \ 1]^\top, \quad \hat{\mathbf{c}} = [w_1 \ w_2 \ \dots \ b_k]^\top. \quad (6b)$$

Then the transfer function $r(z)$ in (4) with the matrices from (6) is the same rational function as the barycentric form (5) with parameters $\{\lambda_j\}_{j=1}^k$, $\{h_j\}_{j=1}^k$, and $\{w_j\}_{j=1}^k$; see, for example, [18].

Throughout this work, we will denote the vector of *numerator basis functions* of the barycentric form as

$$\mathbf{p}(z) = \left[\frac{h_1}{z-\lambda_1} \ \dots \ \frac{h_k}{z-\lambda_k} \right]^\top \in \mathbb{C}^k, \quad (7)$$

the vector of *denominator basis functions* as

$$\mathbf{q}(z) = \left[\frac{1}{z-\lambda_1} \ \dots \ \frac{1}{z-\lambda_k} \right]^\top \in \mathbb{C}^k, \quad (8)$$

and the vector of barycentric weights via

$$\mathbf{w} = [w_1 \ \dots \ w_k]^\top \in \mathbb{C}^k. \quad (9)$$

Then, the barycentric form (5) can be compactly written as

$$r(z; \mathbf{w}) = \frac{n(z; \mathbf{w})}{d(z; \mathbf{w})} = \frac{\mathbf{w}^\top \mathbf{p}(z)}{\mathbf{w}^\top \mathbf{q}(z)}. \quad (10)$$

Note that the dependence of the rational function r as well as the numerator and denominator terms on the barycentric weights \mathbf{w} serves the simplicity of presentation since we will further investigate the effects of different weight choices.

2.3 AAA and the Levy approximation

The AAA algorithm has been established as an efficient and effective approach for the approximation of given data via rational functions [24]. The method is based on a greedy selection of barycentric support points and the Levy approximation [20] to the rational least-squares data fitting problem.

In what follows, we assume that for a general function $H : \mathbb{C} \rightarrow \mathbb{C}$, we have given $M \in \mathbb{N}$ samples of the function evaluation of H in the form

$$\mathbb{D} = \{(z_1, H(z_1)), (z_2, H(z_2)), \dots, (z_M, H(z_M))\}. \quad (11)$$

The objective of AAA is the iterative construction of rational approximations to the given data (11) in the barycentric form

$$r^{(k)}(z; \mathbf{w}^{(k)}) = \frac{n^{(k)}(z; \mathbf{w}^{(k)})}{d^{(k)}(z; \mathbf{w}^{(k)})} = \frac{(\mathbf{w}^{(k)})^\top \mathbf{p}^{(k)}(z)}{(\mathbf{w}^{(k)})^\top \mathbf{q}^{(k)}(z)}, \quad (12)$$

where $k = 0, 1, \dots, k_{\max}$ denotes the iteration index. The iteration may be stopped early when the approximation error between the current rational approximant $r^{(k)}$ and the data \mathbb{D} is below a user-defined tolerance τ . When it is clear from the context, the iteration index k is dropped for simplicity of notation.

The AAA algorithm is initialized with a rational approximant of degree 0. The classical choice for the initialization is the average of the given data,

$$r^{(0)}(z) \equiv \frac{1}{M} \sum_{i=1}^M H(z_i). \quad (13)$$

For $k \geq 1$, AAA then determines the support points and weights of a rational function r in the interpolatory barycentric form (5). At the k -th iteration, the location of the maximum mismatch between the current rational approximant and the data is identified to determine the k -th barycentric support point via

$$\lambda_k = \operatorname{argmax}_{(z_i, H(z_i)) \in \mathbb{D}} |r^{(k-1)}(z_i; \mathbf{w}^{(k-1)}) - H(z_i)|. \quad (14)$$

With the new support point λ_k and the corresponding function value $h_k = H(\lambda_k)$, numerator and denominator bases are updated to

$$\mathbf{p}(z) = \begin{bmatrix} \frac{h_1}{z-\lambda_1} & \dots & \frac{h_{k-1}}{z-\lambda_{k-1}} & \frac{h_k}{z-\lambda_k} \end{bmatrix}^\top \quad \text{and} \quad (15a)$$

$$\mathbf{q}(z) = \begin{bmatrix} \frac{1}{z-\lambda_1} & \dots & \frac{1}{z-\lambda_{k-1}} & \frac{1}{z-\lambda_k} \end{bmatrix}^\top. \quad (15b)$$

Afterwards, AAA aims to use the remaining degrees of freedom via the weights in \mathbf{w} to minimize the least-squares error of the approximation

$$E = \sum_{i=1}^M |r(z_i; \mathbf{w}) - H(z_i)|^2. \quad (16)$$

Since (16) is nonlinear in the unknown weights \mathbf{w} , instead of solving (16), AAA minimizes the corresponding Levy approximation of the error, namely

$$E_{\text{Levy}} = \sum_{i=1}^M |n(z_i; \mathbf{w}) - d(z_i; \mathbf{w})H(z_i)|^2, \quad (17)$$

where n and d are the numerator and denominator of the barycentric form of r . Hence, the weights \mathbf{w} are found via

$$\mathbf{w} = \operatorname{argmin}_{\mathbf{v} \in \mathbb{C}^k} \sum_{i=1}^M |n(z_i; \mathbf{v}) - d(z_i; \mathbf{v})H(z_i)|^2 \quad (18a)$$

$$= \operatorname{argmin}_{\mathbf{v} \in \mathbb{C}^k} \sum_{i=1}^M |\mathbf{v}^\top \mathbf{p}(z_i) - \mathbf{v}^\top \mathbf{q}(z_i)H(z_i)|^2. \quad (18b)$$

The expression in (18) is a homogeneous linear least-squares problem, and thus has the trivial solution $\mathbf{w} = \mathbf{0}$. This is an artifact of the non-uniqueness of the weights in the barycentric form. We follow the original proposition in [24] and circumvent this issue by enforcing that $\|\mathbf{w}\|_2 = 1$.

To effectively solve (18) with the constraint $\|\mathbf{w}\|_2 = 1$, we first note that as a result of the interpolation property of the barycentric form, the approximation errors of r in the support points $\lambda_1, \dots, \lambda_k$ is zero. Therefore, we will exclude the k interpolated data samples from the data set \mathbb{D} for the solution of the linear least-squares problem. For simplicity of presentation, we re-index the remaining (non-interpolated) data samples in \mathbb{D} to be $\{(z_i, H(z_i))\}_{i=1}^{M-k}$. Now, define the Cauchy matrix $\mathbf{C} \in \mathbb{C}^{(M-k) \times k}$ via

$$\mathbf{C}_{i,j} = \frac{1}{z_i - \lambda_j}, \quad \text{for } i = 1, \dots, M-k \quad \text{and } j = 1, \dots, k, \quad (19)$$

define the diagonal matrix of interpolated function values as

$$\mathbf{H} = \text{diag}(h_1, h_2, \dots, h_k) \in \mathbb{C}^{k \times k}, \quad (20)$$

and define the diagonal matrix of non-interpolated data values by

$$\mathbf{G} = \text{diag}(H(z_1), H(z_2), \dots, H(z_{M-k})) \in \mathbb{C}^{(M-k) \times (M-k)}. \quad (21)$$

Then, the solution to (18), with $\|\mathbf{w}\|_2 = 1$, can equivalently be obtained from

$$\mathbf{w} = \underset{\mathbf{v} \in \mathbb{C}^k, \|\mathbf{v}\|_2=1}{\operatorname{argmin}} \|\mathbf{G}\mathbf{C} - \mathbf{C}\mathbf{H}\mathbf{v}\|_2^2. \quad (22)$$

Finally, the solution to (22) is simply given as the k -th right-singular vector of the matrix $\mathbf{G}\mathbf{C} - \mathbf{C}\mathbf{H}$. The complete AAA algorithm is summarized in [Algorithm 1](#).

3 Iterative refinements to the Levy approximation

The Levy approximation (17) to the rational least-squares problem (16) enables the rapid construction of rational approximants in the AAA algorithm. However, the solution to the linearized least-squares problem may not coincide well with the solution to the true rational least-squares problem. To resolve this, we present in this section two iterative refinement approaches for Levy's approximation, which improve the approximation accuracy by solving a sequence of linear least-squares problems.

3.1 Sanathanan-Koerner iteration

In general, for rational functions of the form (10), Levy's approximation to the rational least-squares problem (16) can be derived using the reformulation of the individual error terms in (16) by factoring out the denominators such as

$$\left| \frac{n(z; \mathbf{w})}{d(z; \mathbf{w})} - H(z) \right| = \left| \frac{1}{d(z; \mathbf{w})} \right| |n(z; \mathbf{w}) - d(z; \mathbf{w})H(z)|. \quad (23)$$

Then, Levy's approximation (to the error) is given by

$$\left| \frac{1}{d(z; \mathbf{w})} \right| |n(z; \mathbf{w}) - d(z; \mathbf{w})H(z)| \approx |n(z; \mathbf{w}) - d(z; \mathbf{w})H(z)|, \quad (24)$$

Algorithm 1: Adaptive Antoulas-Anderson (AAA) algorithm.

Input: Data set $\mathbb{D} = \{(z_i, H(z_i))\}_{i=1}^M$, error tolerance τ , maximum degree of rational approximant k_{\max} .

Output: Barycentric parameters $\{h_j\}_{j=1}^k$, $\{\lambda_j\}_{j=1}^k$, $\{w_j\}_{j=1}^k$.

1 Initialize $r^{(0)}(z_i) \equiv \frac{1}{M} \sum_{i=1}^M H(z_i)$, $\mathbf{p}^{(0)} = []$, and $\mathbf{q}^{(0)} = []$.

2 **for** $k = 1, \dots, k_{\max} + 1$ **do**

3 Determine the next support point and function value

$$(\lambda_k, h_k) = \underset{(z_i, H(z_i)) \in \mathbb{D}}{\operatorname{argmax}} |r^{(k-1)}(z_i; \mathbf{w}^{(k-1)}) - H(z_i)|.$$

4 Update the basis vectors with (λ_k, h_k) so that

$$\mathbf{p}^{(k)}(z) = \begin{bmatrix} \frac{h_1}{z-\lambda_1} & \dots & \frac{h_{k-1}}{z-\lambda_{k-1}} & \frac{h_k}{z-\lambda_k} \end{bmatrix}^T,$$

$$\mathbf{q}^{(k)}(z) = \begin{bmatrix} \frac{1}{z-\lambda_1} & \dots & \frac{1}{z-\lambda_{k-1}} & \frac{1}{z-\lambda_k} \end{bmatrix}^T.$$

5 Update the data set $\mathbb{D} \leftarrow \mathbb{D} \setminus \{(\lambda_k, h_k)\}$.

6 Form the matrices $\mathbf{C}, \mathbf{H}, \mathbf{G}$ via (19)–(21).

7 Solve the constrained linear least-squares problem

$$\mathbf{w}^{(k)} = \underset{\mathbf{v} \in \mathbb{C}^k, \|\mathbf{v}\|_2=1}{\operatorname{argmin}} \|(\mathbf{G}\mathbf{C} - \mathbf{C}\mathbf{H})\mathbf{v}\|_2^2.$$

8 **if** $\sum_{i=1}^{M-k} |r^{(k)}(z_i; \mathbf{w}^{(k)}) - H(z_i)|^2 < \tau$ **then break**

9 **end**

that is, the nonlinear objective function (16) is scaled by the reciprocals of the absolute values of the denominator.

In [27], Sanathanan and Koerner developed an iteration scheme (further on referred to as Sanathanan-Koerner iteration or simply SK iteration) that aims to undo the scaling introduced by the Levy approximation (24). In the p -th step of the iteration, for a degree- $(k-1)$ rational function in barycentric form, SK finds new weights $\mathbf{w}_{(p)} \in \mathbb{C}^k$ as minimizer of the weighted linear least-squares error

$$E_{\text{SK}} = \sum_{i=1}^M \frac{1}{|d(z_i; \mathbf{w}_{(p-1)})|^2} |n(z_i; \mathbf{w}_{(p)}) - d(z_i; \mathbf{w}_{(p)})H(z_i)|^2, \quad (25)$$

where the weighting is given by the $d(z_i; \mathbf{w}_{(p-1)})$ using the weights from the previous iteration step. The iteration is initialized with the constant denominator $d(z; \mathbf{w}_{(0)}) \equiv 1$ such that in the first step of SK the solution to the Levy approximation (17) is computed.

The original work [27] describes the numerical procedure with a generic polynomial basis. Here, we present the necessary computations in the interpolatory barycentric form instead. For fixed numerator basis \mathbf{p} and denominator basis \mathbf{q} , at every iteration step $p \geq 1$, the updated weights $\mathbf{w}_{(p)}$ are given by

$$\mathbf{w}_{(p)} = \underset{\mathbf{v} \in \mathbb{C}^k, \|\mathbf{v}\|_2=1}{\operatorname{argmin}} \sum_{i=1}^M \frac{1}{|\mathbf{w}_{(p-1)}^T \mathbf{q}(z_i)|^2} |\mathbf{v}^T \mathbf{p}(z_i) - \mathbf{v}^T \mathbf{q}(z_i)H(z_i)|^2, \quad (26)$$

where the non-uniqueness of the weights in the barycentric form is resolved via the added constraint $\|\mathbf{w}_{(p)}\|_2 = 1$.

Algorithm 2: Sanathanan-Koerner (SK) iteration.

Input: Data set $\mathbb{D} = \{(z_i, H(z_i))\}_{i=1}^{M-k}$, convergence tolerance τ_{SK} , barycentric parameters $\{\lambda_j\}_{j=1}^k$ and $\{h_j\}_{j=1}^k$, maximum number of iterations p_{\max} .

Output: Barycentric weights \mathbf{w} .

- 1 Initialize $d_{(0)}(z) \equiv 1$, $\mathbf{e}_{\ell_2} = []$, and $\mathbf{w}_{(0)} = \mathbf{0}$.
- 2 Form the matrices $\mathbf{C}, \mathbf{H}, \mathbf{G}$ via (19)–(21).
- 3 **for** $p = 1, \dots, p_{\max}$ **do**
- 4 Compute the weighting matrix $\mathbf{D}_{(p-1)}$ using (27).
- 5 Solve the constrained linear least-squares problem
$$\mathbf{w}_{(p)} = \underset{\mathbf{v} \in \mathbb{C}^k, \|\mathbf{v}\|_2=1}{\operatorname{argmin}} \|\mathbf{D}_{(p-1)}(\mathbf{G}\mathbf{C} - \mathbf{C}\mathbf{H})\mathbf{v}\|_2^2.$$
- 6 Expand the error vector $\mathbf{e}_{\ell_2} \leftarrow \left[\mathbf{e}_{\ell_2} \quad \sum_{i=1}^{M-k} |r(z_i; \mathbf{w}_{(p)}) - H(z_i)|^2 \right]$.
- 7 **if** $\|\mathbf{w}_{(p)} - \mathbf{w}_{(p-1)}\|_2 < \tau_{\text{SK}}$ **then break**
- 8 **end**
- 9 Find the index p_{best} of the smallest entry in \mathbf{e}_{ℓ_2} .
- 10 Set $\mathbf{w} \leftarrow \mathbf{w}_{(p_{\text{best}})}$.

Similar to the Levy approximated least-squares problem, we may solve (26) via a reformulation into matrix form. To this end, we construct the same matrices $\mathbf{C} \in \mathbb{C}^{(M-k) \times k}$, $\mathbf{H} \in \mathbb{C}^{(M-k) \times (M-k)}$, and $\mathbf{G} \in \mathbb{C}^{k \times k}$ as in (19)–(21), and we define the new diagonal weighting matrix

$$\mathbf{D}_{(p-1)} = \operatorname{diag} \left(\frac{1}{|d(z_1; \mathbf{w}_{(p-1)})|}, \dots, \frac{1}{|d(z_{M-k}; \mathbf{w}_{(p-1)})|} \right) \in \mathbb{R}^{(M-k) \times (M-k)}. \quad (27)$$

Then, the solution to (26) is equivalent to the solution to

$$\mathbf{w}_{(p)} = \underset{\mathbf{v} \in \mathbb{C}^k, \|\mathbf{v}\|_2=1}{\operatorname{argmin}} \|\mathbf{D}_{(p-1)}(\mathbf{G}\mathbf{C} - \mathbf{C}\mathbf{H})\mathbf{v}\|_2^2, \quad (28)$$

which is given by the k -th right-singular vector of the matrix $\mathbf{D}_{(p-1)}(\mathbf{G}\mathbf{C} - \mathbf{C}\mathbf{H})$.

The SK iteration is considered to have converged when the change in the weight vectors of consecutive iteration steps is small enough. In general, there are no convergence guarantees for the SK iteration, and the approach has been observed to not necessarily converge for all possible choices of barycentric support points and function values. Therefore, in our implementation of the SK iteration, we additionally evaluate the rational least-squares error (16) at every iteration step and return weights $\mathbf{w}_{(p)}$ corresponding to the lowest rational least-squares error of all computed iterates. The SK iteration is summarized in [Algorithm 2](#).

Remark 1. The coefficient matrix in (28) is known to become highly ill-conditioned. A variety of approaches has been explored to resolve this conditioning issue in the standard SK iteration leading, for example, to the vector fitting method [16], the stabilized SK iteration [17], or the orthogonal rational approximation [21]. However, all of these methods rely on the ability to change the basis vectors (7) and (8) of the rational function at each iteration. As we require a specific barycentric basis chosen to enforce interpolation conditions, these techniques are not applicable to this work.

3.2 Whitfield's iteration

Another refinement procedure for the solution of the rational least-squares problem was proposed by Whitfield in [28]. Here, we re-derive the approach using the barycentric representation (5) while the original work used a generic polynomial basis. Similar to the SK iteration, Whitfield's (WF) iteration seeks to minimize the rational least-squares error (16) by solving a sequence of linear least-squares approximations starting from an initial weight vector $\mathbf{w}_{(0)}$. In the following, we assume that $d(z_i; \mathbf{w}) = \mathbf{w}^\top \mathbf{q}(z_i) \neq 0$ holds for all z_i in the sampled data set \mathbb{D} from (11).

In the p -th step of the WF iteration, we form a linear approximation of the rational function r along the weights centered at the previous weights $\mathbf{w}_{(p-1)}$. This particular linearization of the rational function r is given by

$$r(z; \mathbf{w}) \approx r(z; \mathbf{w}_{(p-1)}) + \left(\frac{\partial r(z; \mathbf{w})}{\partial \mathbf{w}} \Big|_{\mathbf{w}=\mathbf{w}_{(p-1)}} \right)^\top (\mathbf{w} - \mathbf{w}_{(p-1)}). \quad (29)$$

Therein, the partial derivative $r(z; \mathbf{w}) = (\mathbf{w}^\top \mathbf{p}(z)) / (\mathbf{w}^\top \mathbf{q}(z))$ with respect to the weights \mathbf{w} takes the form

$$\frac{\partial r(z; \mathbf{w})}{\partial \mathbf{w}} = \frac{1}{d(z; \mathbf{w})} (\mathbf{p}(z) - r(z; \mathbf{w}) \mathbf{q}(z)). \quad (30)$$

Inserting (30) into (29) then yields the linear approximation of the form

$$r(z; \mathbf{w}) \approx r(z; \mathbf{w}_{(p-1)}) + \left(\frac{1}{d(z; \mathbf{w}_{(p-1)})} (\mathbf{p}(z) - r(z; \mathbf{w}_{(p-1)}) \mathbf{q}(z)) \right)^\top (\mathbf{w} - \mathbf{w}_{(p-1)}) \quad (31a)$$

$$= \frac{1}{d(z; \mathbf{w}_{(p-1)})} (n(z; \mathbf{w}) - r(z; \mathbf{w}_{(p-1)}) d(z; \mathbf{w}) + n(z; \mathbf{w}_{(p-1)})). \quad (31b)$$

Finally, substituting the expression (31b) in the rational least-squares error (16) gives the new linear least-squares error

$$\begin{aligned} E_{WF} &= \sum_{i=1}^M \frac{1}{|d(z_i; \mathbf{w}_{(p-1)})|^2} \left| n(z_i; \mathbf{w}) - r(z_i; \mathbf{w}_{(p-1)}) d(z_i; \mathbf{w}) \right. \\ &\quad \left. + n(z_i; \mathbf{w}_{(p-1)}) - d(z_i; \mathbf{w}_{(p-1)}) H(z_i) \right|^2. \end{aligned} \quad (32)$$

Then, for every step $p \geq 1$ of the iteration, the new weights $\mathbf{w}_{(p)}$ are calculated as the solution to

$$\begin{aligned} \mathbf{w}_{(p)} = \operatorname{argmin}_{\mathbf{v} \in \mathbb{C}^k} \sum_{i=1}^M \frac{1}{|\mathbf{w}_{(p-1)}^\top \mathbf{q}(z_i)|^2} &\left| \mathbf{v}^\top \mathbf{p}(z_i) - \frac{\mathbf{w}_{(p-1)}^\top \mathbf{p}(z_i)}{\mathbf{w}_{(p-1)}^\top \mathbf{q}(z_i)} \mathbf{v}^\top \mathbf{q}(z_i) \right. \\ &\quad \left. + \mathbf{w}_{(p-1)}^\top \mathbf{p}(z_i) - \mathbf{w}_{(p-1)}^\top \mathbf{q}(z_i) H(z_i) \right|^2. \end{aligned} \quad (33)$$

We note that the least-squares error in (32) depends on both the previous numerator $n(z; \mathbf{w}_{(p-1)})$ and the previous denominator $d(z; \mathbf{w}_{(p-1)})$. Initializing both of these quantities for the iteration is a non-trivial task. In particular, initializing both numerator and denominator identical to 1 does not result in the Levy approximation (17). We explore initialization strategies for the WF iteration later in Section 4.3.

While both the Levy approximation and SK iteration require the solution of constrained homogeneous linear least-squares problems (22) and (28), the WF iteration calls for the

solution of non-homogeneous linear least-squares problems of the form (33) and hence does not yield a trivial solution. However, (33) does not have a unique solution either due to the non-uniqueness of the weights in the barycentric form (5). To resolve the non-uniqueness of the least-squares solution in the WF iteration, we enforce the first weight vector entry to be 1, i.e., we add the constraint

$$[\mathbf{w}_{(p)}]_1 = 1. \quad (34)$$

For the solution of (33) with the constraint (34), we assemble the weight matrix $\mathbf{D}_{(p-1)}$ as in (27), and define the new matrix $\mathbf{F}_{(p-1)} \in \mathbb{C}^{(M-k) \times k}$ entrywise via

$$[\mathbf{F}_{(p-1)}]_{i,j} = \frac{h_j}{z_i - \lambda_j} - r(z_i; \mathbf{w}_{(p-1)}) \frac{1}{z_i - \lambda_j}, \quad (35)$$

for $i = 1, \dots, M - k$ and $j = 1, \dots, k$, and we define the vector $\mathbf{b}_{(p-1)} \in \mathbb{C}^{(M-k)}$ as

$$[\mathbf{b}_{(p-1)}]_i = -n(z_i; \mathbf{w}_{(p-1)}) + d(z_i; \mathbf{w}_{(p-1)}) H(z_i). \quad (36)$$

for $i = 1, \dots, M - k$. Similar to the construction of $\mathbf{D}_{(p-1)}$ in (27), the data samples used in (35) and (36) do not include the interpolated data samples that are used as parameters in the barycentric form. Using these matrices, the solution to (33) with the constraint (34) is given by

$$\mathbf{w}_{(p)} = \underset{\mathbf{v} \in \mathbb{C}^k, v_1=1}{\operatorname{argmin}} \left\| \mathbf{D}_{(p-1)} \left([\mathbf{F}_{(p-1)}]_{:,2:k} [\mathbf{v}]_{2:k} - (\mathbf{b}_{(p-1)} - [\mathbf{F}_{(p-1)}]_{:,1}) \right) \right\|_2^2, \quad (37)$$

where $[\mathbf{F}_{(p-1)}]_{:,2:k}$ denotes the last $k - 1$ columns of the matrix $\mathbf{F}_{(p-1)}$, while $[\mathbf{F}_{(p-1)}]_{:,1}$ denotes the first column of $\mathbf{F}_{(p-1)}$, and $[\mathbf{v}]_{2:k}$ marks the last $k - 1$ rows of the vector \mathbf{v} . Equation (37) can be seen as a classical unconstrained non-homogeneous weighted linear least-squares problem in $k - 1$ variables, and it can be solved by any off-the-shelf solver.

Similar to the case of the SK iteration, there are no convergence guarantees for the WF iteration. As such, we employ the same strategy in the implementation of the WF iteration to save the rational least-squares errors (16) at every iteration step and then return the weights corresponding to the smallest error. The WF iteration is outlined in [Algorithm 3](#).

4 Nonlinear least-squares refinement for AAA

In principle, the two steps performed in the classical AAA are the greedy selection of the next interpolation point from the data and the subsequent fit of the barycentric weights using the Levy approximation of the rational least-squares problem. We propose the replacement of the Levy approximation in AAA by the iterative refinement methods discussed earlier. In this section, we first describe our proposed new AAA-type algorithm before we analyze the potential effectiveness of the different refinement methods integrated into our proposed algorithm for the solution of the true nonlinear least-squares problem.

4.1 Algorithm description

Using the machinery outlined in [Section 3](#), we present our Nonlinear Least-squares AAA algorithm (NL-AAA) in [Algorithm 4](#). While the first steps of [Algorithm 1](#) (AAA) and [Algorithm 4](#) are identical, the solution to the constrained linear least-squares problem in [Algorithm 1](#) is replaced by Lines 6–12 in [Algorithm 4](#). First, a refined set of weights

Algorithm 3: Whitfield's (WF) iteration.

Input: Data set $\mathbb{D} = \{(z_i, H(z_i))\}_{i=1}^{M-k}$, convergence tolerance τ_{WF} , barycentric parameters $\{\lambda_j\}_{j=1}^k$ and $\{h_j\}_{j=1}^k$, initial weights $\mathbf{w}_{(0)}$, maximum number of iterations p_{\max} .

Output: Barycentric weights \mathbf{w} .

1 Initialize $\mathbf{e}_{\ell_2} = []$.

2 **for** $p = 1, \dots, p_{\max}$ **do**

3 Construct $\mathbf{D}_{(p-1)}$, $\mathbf{F}_{(p-1)}$ and $\mathbf{b}_{(p-1)}$ using (27), (35), and (36).

4 Solve the linear least-squares problem

$$\mathbf{w}_{(p)} = \underset{\mathbf{v} \in \mathbb{C}^k, \mathbf{v}_1=1}{\operatorname{argmin}} \left\| \mathbf{D}_{(p-1)} \left([\mathbf{F}_{(p-1)}]_{:,2:k} [\mathbf{v}]_{2:k} - (\mathbf{b}_{(p-1)} - [\mathbf{F}_{(p-1)}]_{:,1}) \right) \right\|_2^2.$$

5 Expand the error vector $\mathbf{e}_{\ell_2} \leftarrow \left[\mathbf{e}_{\ell_2} \quad \sum_{i=1}^{M-k} |r(z_i; \mathbf{w}_{(p)}) - H(z_i)|^2 \right]$.

6 **if** $\|\mathbf{w}_{(p)} - \mathbf{w}_{(p-1)}\|_2 < \tau_{WF}$ **then break**

7 **end**

8 Find the index p_{best} of the smallest entry in \mathbf{e}_{ℓ_2} .

9 Set $\mathbf{w} \leftarrow \mathbf{w}_{(p_{\text{best}})}$.

\mathbf{w}_{SK} is computed using the SK iteration from [Algorithm 2](#) in [Algorithm 4](#). Then, a single iteration step of the WF iteration from [Algorithm 3](#) is performed in [Algorithm 4](#) using the previous set of weights extended by zero, $[(\mathbf{w}^{(k-1)})^\top 0]^\top$, as initialization to compute an alternative set of weights $\mathbf{w}_{(1)}$. Afterwards, the two weight vectors are compared in terms of the corresponding approximation errors to determine how to initialize a complete run of the WF iteration. If \mathbf{w}_{SK} gives the smaller error, then [Algorithm 3](#) is run with the initialization $\mathbf{w}_{(0)} = \mathbf{w}_{SK}$ to compute $\mathbf{w}^{(k)}$. Otherwise, [Algorithm 3](#) is run with the initialization $[(\mathbf{w}^{(k-1)})^\top 0]^\top$. The motivation for this specific initialization strategy and alternative strategies in the case that the iterative refinement strategies fail are explained in detail in [Section 4.3](#).

In terms of additional computational costs for [Algorithm 4](#) compared to [Algorithm 1](#), we note that the main costs in both algorithms stem from the solution of linear least-squares problems. Thereby, in the case that neither refinement procedure converges early, [Algorithm 4](#) is solving two sequences of linear least-squares problems of the same dimensions as the single one in [Algorithm 1](#) making [Algorithm 4](#) computationally more expensive than the classical method in terms of computation time. However, the amount of additional computation time is bounded by the maximum number of iterations in the refinement procedures so that each step of [Algorithm 4](#) is at most $2p_{\max}$ times as expensive as the corresponding step in [Algorithm 1](#). Therefore, our proposed method lies in the same order of computational complexity as the original method. As we will show in various numerical examples, NL-AAA typically achieves a given tolerance at a lower degree than AAA; thus even though the individual iteration step is computationally more expensive, in many cases NL-AAA achieves the given target tolerance with a smaller number of iteration steps.

4.2 Analysis of the approximation and refinement methods

In this section, we provide the theoretical justification for the design of our proposed NL-AAA algorithm ([Algorithm 4](#)). After a quick introduction of the Wirtinger calculus, we derive and analyze the gradients of the approximations done by Levy, SK, and WF. While

Algorithm 4: Nonlinear Least-squares AAA (NL-AAA) algorithm.

Input: Data set $\mathbb{D} = \{(z_i, H(z_i))\}_{i=1}^M$, error tolerance τ , maximum number of refinement iterations p_{\max} , refinement convergence tolerances τ_{SK} and τ_{WF} , maximum degree of rational approximant k_{\max} .

Output: Barycentric parameters $\{h_j\}_{j=1}^k$, $\{\lambda_j\}_{j=1}^k$, $\{w_j\}_{j=1}^k$.

1 Initialize $r^{(0)}(z_i) \equiv \frac{1}{M} \sum_{i=1}^M H(z_i)$, $\mathbf{p}^{(0)} = []$, and $\mathbf{q}^{(0)} = []$.

2 **for** $k = 1, \dots, k_{\max} + 1$ **do**

3 Determine the next support point and function value

$$(\lambda_k, h_k) = \underset{(z_i, H(z_i)) \in \mathbb{D}}{\operatorname{argmax}} |r^{(k-1)}(z_i; \mathbf{w}^{(k-1)}) - H(z_i)|.$$

4 Update the basis vectors with (λ_k, h_k) so that

$$\mathbf{p}^{(k)}(z) = \begin{bmatrix} \frac{h_1}{z-\lambda_1} & \dots & \frac{h_{k-1}}{z-\lambda_{k-1}} & \frac{h_k}{z-\lambda_k} \end{bmatrix}^T,$$

$$\mathbf{q}^{(k)}(z) = \begin{bmatrix} \frac{1}{z-\lambda_1} & \dots & \frac{1}{z-\lambda_{k-1}} & \frac{1}{z-\lambda_k} \end{bmatrix}^T.$$

5 Update the data set $\mathbb{D} \leftarrow \mathbb{D} \setminus \{(\lambda_k, h_k)\}$.

6 Compute \mathbf{w}_{SK} via p_{\max} iterations of [Algorithm 2](#) and tolerance τ_{SK} .

7 Compute $\mathbf{w}_{(1)}$ via 1 iteration of [Algorithm 3](#) using $\left[(\mathbf{w}^{(k-1)})^T \ 0 \right]^T$.

8 **if** $\sum_{i=1}^{M-k} |r^{(k)}(z_i; \mathbf{w}_{\text{SK}}) - H(z_i)|^2 < \sum_{i=1}^{M-k} |r^{(k)}(z_i; \mathbf{w}_{(1)}) - H(z_i)|^2$ **then**

9 Compute the weights $\mathbf{w}^{(k)}$ via p_{\max} iterations of [Algorithm 3](#) using $\mathbf{w}_{(0)} = \mathbf{w}_{\text{SK}}$ and tolerance τ_{WF} .

10 **else**

11 Compute the weights $\mathbf{w}^{(k)}$ via p_{\max} iterations of [Algorithm 3](#) using $\mathbf{w}_{(0)} = \left[(\mathbf{w}^{(k-1)})^T \ 0 \right]^T$ and tolerance τ_{WF} .

12 **end**

13 **if** $\sum_{i=1}^{M-k} |r^{(k)}(z_i; \mathbf{w}^{(k)}) - H(z_i)|^2 < \tau$ **then break**

14 **end**

all these approaches strive to reduce the rational least-squares error [\(16\)](#), we show that only WF minimizes this particular error. In contrast to the work in [\[28\]](#), we rigorously treat the nonanalytic error criteria using the barycentric representation [\(5\)](#) and also provide additional analysis.

4.2.1 Wirtinger calculus

Our main tool for the derivation of the gradients of the error function [\(16\)](#) is the Wirtinger calculus [\[29\]](#). As the objective function and approximations to it are in general mappings from \mathbb{C}^M to \mathbb{R} , they are not complex analytic and hence cannot be differentiated in the notion of classical complex derivatives. However, these functions are differentiable using the Wirtinger calculus, which was specifically designed as a calculus for functions which are not complex-differentiable when regarded as functions from \mathbb{C}^M to \mathbb{C} (resp. \mathbb{R}), but are real-differentiable when regarded as functions from \mathbb{R}^{2M} to \mathbb{R}^2 (resp. \mathbb{R}). To this end, the Wirtinger calculus re-interprets a function $f : \mathbb{C}^M \rightarrow \mathbb{R}$ that depends on the complex variable $\mathbf{z} \in \mathbb{C}^M$ as a function of \mathbf{z} and $\bar{\mathbf{z}}$, where \mathbf{z} and $\bar{\mathbf{z}}$ are treated as independent variables. Equivalently, the function f can be considered as a function of the real and

imaginary parts of the complex variable \mathbf{z} ; see [19]. Then, two gradients are defined based on the partial derivatives of the function f with respect to the real and imaginary parts of the variable \mathbf{z} : the Wirtinger derivative denoted by $\frac{d}{d\mathbf{z}}f(\mathbf{z}, \bar{\mathbf{z}})$ and the conjugate Wirtinger derivative denoted as $\frac{d}{d\bar{\mathbf{z}}}f(\mathbf{z}, \bar{\mathbf{z}})$; see [29]. In the case that the Wirtinger derivative or conjugate Wirtinger derivative is $\mathbf{0}$, the function f is at a stationary point. Furthermore, since in this work we differentiate only real-valued error functions, the following identity holds

$$\frac{d f(\mathbf{z}, \bar{\mathbf{z}})}{d \bar{\mathbf{z}}} = \overline{\frac{d f(\mathbf{z}, \bar{\mathbf{z}})}{d \mathbf{z}}}. \quad (38)$$

Consequently, it is sufficient for us to compute only the Wirtinger derivatives of our error functions in this work. For further information on the Wirtinger calculus, we refer the reader to the collection of lecture notes [19].

4.2.2 Wirtinger derivatives of error functions

With the Wirtinger calculus at hand, we provide in this section the gradients of the nonlinear rational least-squares error criterion (16) and the approximations to that least-squares error done in (17) (Levy), (25) (SK), and (32) (WF). By comparison of the different gradients, we will see that only WF upon convergence truly minimizes the objective of interest (16). However, the gradients of the Levy approximation and SK will reveal in which cases the results of these two approximations are *nearly* optimal.

We begin with the Wirtinger derivative of the nonlinear least-squares error in the following lemma.

Lemma 1. *The Wirtinger derivative of the nonlinear rational least-squares error (16) with respect to the barycentric weights \mathbf{w} is given by*

$$\frac{d E}{d \mathbf{w}} = \sum_{i=1}^M \frac{1}{d(z_i; \mathbf{w})} (\mathbf{p}(z_i) - r(z_i; \mathbf{w}) \mathbf{q}(z_i)) \overline{(r(z_i; \mathbf{w}) - H(z_i))}. \quad (39)$$

Proof. The result directly follows from applying the partial derivative formula (30) to the nonlinear rational least-squares error (16). \square

The derivative given in (39) needs to vanish at the stationary points of the nonlinear rational least-squares error. In contrast to that, the following theorem provides the Wirtinger derivatives for the approximations used in the different solution procedures from above, namely Levy, SK, and WF.

Theorem 1. *The Wirtinger derivative of the Levy approximation error criterion (17) with respect to the barycentric weights \mathbf{w} is given by*

$$\frac{d E_{\text{Levy}}}{d \mathbf{w}} = \sum_{i=1}^M (\mathbf{p}(z_i) - H(z_i) \mathbf{q}(z_i)) \overline{(n(z_i; \mathbf{w}) - d(z_i; \mathbf{w}) H(z_i))}. \quad (40)$$

In the case that the SK iteration converges, the Wirtinger derivative of the SK error criterion (25) in the corresponding fixed point with respect to the barycentric weights \mathbf{w} is given by

$$\frac{d E_{\text{SK}}}{d \mathbf{w}} = \sum_{i=1}^M \frac{1}{d(z_i; \mathbf{w})} (\mathbf{p}(z_i) - H(z_i) \mathbf{q}(z_i)) \overline{(r(z_i; \mathbf{w}) - H(z_i))}. \quad (41)$$

Finally, if the WF iteration converges, then the Wirtinger derivative of the WF error criterion (32) in the corresponding fixed point with respect to the barycentric weights \mathbf{w} is given by

$$\frac{d E_{WF}}{d \mathbf{w}} = \sum_{i=1}^M \frac{1}{d(z_i; \mathbf{w})} (\mathbf{p}(z_i) - r(z_i; \mathbf{w}) \mathbf{q}(z_i)) \overline{(r(z_i; \mathbf{w}) - H(z_i))}. \quad (42)$$

Proof. Starting with the Levy approximation in (17), we can rewrite this expression as

$$E_{Levy} = \sum_{i=1}^M (n(z_i; \mathbf{w}) - d(z_i; \mathbf{w}) H(z_i)) \overline{(n(z_i; \mathbf{w}) - d(z_i; \mathbf{w}) H(z_i))}. \quad (43)$$

Computing the Wirtinger derivative of this with respect to \mathbf{w} only affects the first term in the product, which results in (40). For the SK iteration, we have in the p -th step the error expression

$$E_{SK} = \sum_{i=1}^M \frac{1}{|d(z_i; \mathbf{w}_{(p-1)})|^2} |n(z_i; \mathbf{w}) - d(z_i; \mathbf{w}) H(z_i)|^2. \quad (44)$$

We note that the variable weights only appear in the absolute value of the error but not in the pre-multiplied fraction. As in (43), we can split the absolute value into the multiplication with the conjugate expression and, as a result, the Wirtinger derivative of (44) is given by

$$\frac{d E_{SK}}{d \mathbf{w}} = \sum_{i=1}^M \frac{1}{|d(z_i; \mathbf{w}_{(p-1)})|^2} (\mathbf{p}(z_i) - H(z_i) \mathbf{q}(z_i)) \overline{(n(z_i; \mathbf{w}) - H(z_i) d(z_i; \mathbf{w}))}. \quad (45)$$

In the case that the SK iteration converges, we have that $\mathbf{w}_{(p-1)} = \mathbf{w}_{(p)}$. Then, the expression in (45) can be simplified into (41). Finally, for the WF iteration in the p -th step, we have the error expression

$$\begin{aligned} E_{WF} = & \sum_{i=1}^M \frac{1}{|d(z_i; \mathbf{w}_{(p-1)})|^2} |n(z_i; \mathbf{w}) - r(z_i; \mathbf{w}_{(p-1)}) d(z_i; \mathbf{w}) \\ & + n(z_i; \mathbf{w}_{(p-1)}) - d(z_i; \mathbf{w}_{(p-1)}) H(z_i)|^2, \end{aligned} \quad (46)$$

where $\mathbf{w}_{(p-1)}$ are as in SK the weights obtained in the previous step and independent of the variable \mathbf{w} . Using the same rewriting of the absolute value as in (43), the Wirtinger derivative of (46) is given by

$$\begin{aligned} \frac{d E_{WF}}{d \mathbf{w}} = & \sum_{i=1}^M \frac{1}{|d(z_i; \mathbf{w}_{(p-1)})|^2} (\mathbf{p}(z_i) - r(z_i; \mathbf{w}_{(p-1)}) \mathbf{q}(z_i)) \overline{(n(z_i; \mathbf{w})} \\ & \overline{- r(z_i; \mathbf{w}_{(p-1)}) d(z_i; \mathbf{w}) + n(z_i; \mathbf{w}_{(p-1)}) - d(z_i; \mathbf{w}_{(p-1)}) H(z_i))}. \end{aligned} \quad (47)$$

In the case that the WF iteration converges so that $\mathbf{w}_{(p-1)} = \mathbf{w}_{(p)}$, the derivative in (47) can be rewritten as (42). This concludes the proof. \square

It can immediately be verified that the gradients in (39) and (42) are identical. Thus, if the WF iteration converges, it returns a stationary point of the rational least-squares error with respect to the barycentric weights \mathbf{w} as intended by the iteration. The same cannot be said for the Levy approximation and SK. In the following, we will compare these gradients with the one for the rational least-squares problem to provide further insights into these approximations.

4.2.3 Analysis of error derivatives for Levy and SK

As the expression in (41) is visibly very similar to (39), we begin our analysis with the SK iteration. Comparing the two expressions reveals the only difference being that in (39), the vector of denominator basis functions $\mathbf{q}(z_i)$ is weighted by the rational function $r(z_i; \mathbf{w})$, while in (41) it is weighted by the given data $H(z_i)$. Hence, we expect that if the SK iteration results in a rational approximant $r(z; \mathbf{w})$, which approximates the given data in \mathbb{D} well in the sense that

$$|r(z_i; \mathbf{w}) - H(z_i)| \text{ is small, for } i = 1, \dots, M, \quad (48)$$

then $r(z; \mathbf{w})$ should be nearly optimal in the true, rational error (16). Conversely, if $r(z; \mathbf{w})$ is an insufficient approximation to the data in \mathbb{D} , i.e., it produces a large approximation error, we would expect $r(z; \mathbf{w})$ to be further away from optimality in the nonlinear error (16).

Let us consider these observations in the context of numerical procedures that construct rational approximations such as Algorithms 1 and 4. In early iterations, when the degree of the rational approximant is small and large approximation errors are expected, we would not expect the SK iteration to yield close-to-optimal approximations. On the other hand, for larger degree rational approximations, when the approximation errors are expected to be small so that (48) is likely to hold, we would expect the SK iteration to yield near-optimal approximation results. Furthermore, we note that these observations yield a strong motivation for the greedy interpolation step in both Algorithms 1 and 4. Thereby, the worst case approximation error of the rational approximation is set to zero in every iteration step, which is highly advantageous for satisfying the condition (48).

Proceeding to the Levy approximation, we see that after some algebraic manipulations, the derivative in (40) can be rewritten as

$$\frac{d E_{\text{Levy}}}{d \mathbf{w}} = \sum_{i=1}^M |d(z_i; \mathbf{w})|^2 \left(\frac{1}{d(z_i; \mathbf{w})} (\mathbf{p}(z_i) - H(z_i) \mathbf{q}(z_i)) \overline{(r(z_i; \mathbf{w}) - H(z_i))} \right). \quad (49)$$

Comparing (49) to (39) reveals two major differences: First, the terms in (49) are weighted by the denominator $|d(z_i; \mathbf{w})|^2$ and second, as previously for SK, the vector of denominator basis functions $\mathbf{q}(z_i)$ is weighted by $H(z_i)$ rather than $r(z_i; \mathbf{w})$.

Following the latter point, parts of the analysis for the SK iteration also hold for the Levy approximation. If the weights \mathbf{w} obtained via the Levy approximation result in a poor approximation to the data in \mathbb{D} , then we expect that the rational $r(z; \mathbf{w})$ approximation is far from optimal. Beyond that, the weighting by $|d(z_i; \mathbf{w})|^2$ in (49) acts as another error source concerning optimality, which we now examine in detail.

Let \mathbf{w}_* be the solution to the linear least-squares problem (22), in other words, the weights that minimize the Levy error criterion (17). In the case that $|d(z_i; \mathbf{w}_*)| \equiv d \in \mathbb{C}$, for $i = 1, 2, \dots, M$, then we have that

$$\mathbf{0} = \frac{d E_{\text{Levy}}}{d \mathbf{w}} \Big|_{\mathbf{w}=\mathbf{w}_*} = M |d|^2 \frac{d E_{\text{SK}}}{d \mathbf{w}} \Big|_{\mathbf{w}=\mathbf{w}_*}. \quad (50)$$

Hence, when $|d(z_i; \mathbf{w}_*)|$ is constant, then minimizers of the Levy approximation are also the minimizers in the SK iteration and both approaches provide the same level of accuracy. However, in the case that $|d(z_i; \mathbf{w}_*)|$ is not constant but varies by several orders of magnitude over the data \mathbb{D} , we expect the minimizers of the Levy approximation to be far from the optimal approximation in the rational least-squares error (16).

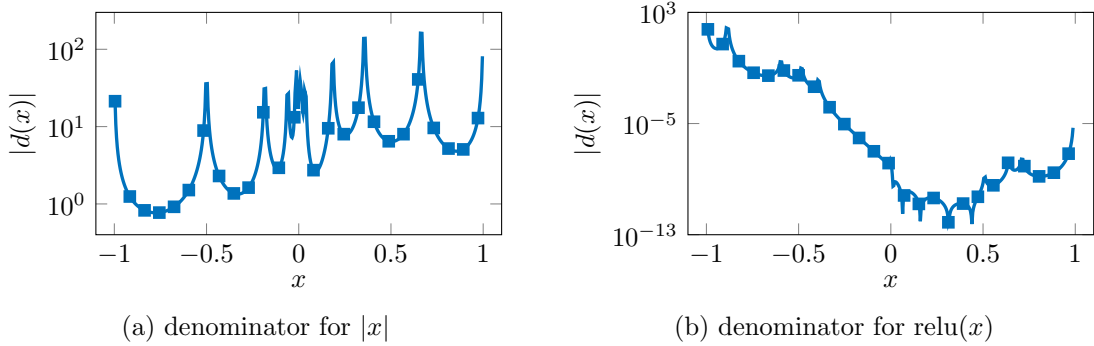


Figure 2: Denominator functions of degree $k = 14$ of the AAA approximations to $|x|$ and $\text{relu}(x)$ on the real interval $[-1, 1]$: While the variation of the approximating denominator for $|x|$ is constrained to only two order of magnitude, the denominator varies nearly 17 orders of magnitude in the approximation of $\text{relu}(x)$.

We are now in a position to justify the differences in the performances of AAA and NL-AAA for the two example functions in Figure 1. As seen in Figure 1b, AAA struggles at iteration $k = 14$ to approximate $\text{relu}(x)$ while NL-AAA already provides a normalized ℓ_2 error of less than 10^{-5} . In contrast, both AAA and NL-AAA are capable of constructing suitably accurate approximations to $|x|$ at iteration $k = 14$; see Fig. 1a. As suggested by our analysis, we examine the variation in the denominator of function $d(z; \mathbf{w})$ constructed via AAA for $|x|$ and $\text{relu}(x)$ at iteration 14 over the real approximation interval $[-1, 1]$ shown in Figure 2. In Figure 2a, we see that while the denominator of the AAA approximation to $|x|$ is not constant, its variation is constrained to only two orders of magnitude. However, on the other side, we see in Figure 2b that the denominator of the AAA approximation for $\text{relu}(x)$ shows nearly 17 orders of magnitude in variation. Correspondingly, the AAA approximation to $|x|$ is nearly as good as the locally optimal NL-AAA approximation in Figure 1a, and the AAA approximation to $\text{relu}(x)$ is clearly not close to optimal in Figure 1b.

4.3 Initializations for Whitfield's iteration

As with all nonlinear optimization methods, a good initialization is essential for the success of the method. In this section, we detail our initialization strategy for the WF iteration in the NL-AAA algorithm, which ensures monotonic error decay.

It has been observed in [11] that in some situations, initializing the WF iteration with the output of the SK iteration can lead to better convergence of WF. This is supported by our previous analysis of the gradients in Section 4.2.3 in so far that the SK iteration may provide nearly optimal results in the case of small approximation errors. We note that since the first step of the SK iteration computes the Levy approximation, this initialization strategy also implicitly considers the use of the Levy approximation, in particular when the iterate of SK with the smallest approximation error is used for the initialization. While this may work well, we have also observed in several numerical instances that the weights $\mathbf{w}_{(p)}^{(k)}$ computed during all the SK iteration steps only increased the nonlinear least-squares error so that

$$\sum_{i=1}^M \left| H(z_i) - \frac{(\mathbf{w}^{(k-1)})^\top \mathbf{p}^{(k-1)}(z_i)}{(\mathbf{w}^{(k-1)})^\top \mathbf{q}^{(k-1)}(z_i)} \right|^2 < \sum_{i=1}^M \left| H(z_i) - \frac{(\mathbf{w}_{(p)}^{(k)})^\top \mathbf{p}^{(k)}(z_i)}{(\mathbf{w}_{(p)}^{(k)})^\top \mathbf{q}^{(k)}(z_i)} \right|^2, \quad (51)$$

for all $p = 0, 1, \dots, p_{\max}$. To avoid the initialization of **WF** with such an unintended choice of weights, we propose to use the following initialization vector in the cases when the **SK** iteration does not yield any suitable results:

$$\begin{bmatrix} (\mathbf{w}^{(k-1)})^T & 0 \end{bmatrix}^T. \quad (52)$$

These are the weights from the previous **NL-AAA** step appended by 0. Thus, the initialization (52) begins the **WF** iteration with a rational function that is equal to the final rational approximation from the previous iteration step.

While we have observed that one of these two initialization strategies lead to a suitable decrease in the approximation error in most cases, it is still potentially possible that the **WF** iteration does not decrease the error at any iteration. In this case, in order to preserve the error monotonicity of the **NL-AAA** method, we set the weights to

$$\mathbf{w}^{(k)} = \begin{bmatrix} (\mathbf{w}^{(k-1)})^T & 0 \end{bmatrix}^T. \quad (53)$$

While this choice does preserve monotonicity, it naturally leads to a problem in the greedy interpolation step, which can cause stagnation of the **NL-AAA** algorithm. Specifically, if the weights at iteration k are chosen according to (53), then we are effectively eliminating the contribution of the k -th interpolation point from the error behavior of the approximation. In typical scenarios, this leads to the next support point λ_{k+1} to be chosen adjacent or at least close to the previous support point λ_k such that $\mathbf{q}^{(k+1)}$ and $\mathbf{p}^{(k+1)}$ are not much more expressive than $\mathbf{q}^{(k)}$ and $\mathbf{p}^{(k)}$ leading to the stagnation of **NL-AAA**. The key to overcoming this issue is to change the error measure for the greedy selection step whenever the weights are chosen as (53). We propose two options here. First, we recommend switching the original deterministic greedy selection

$$(\lambda_k, h_k) = \underset{(z_i, H(z_i)) \in \mathbb{D}}{\operatorname{argmax}} |r(z_i; \mathbf{w}^{(k-1)}) - H(z_i)| \quad (54)$$

to a probabilistic greedy selection. Thereby, we sample (λ_k, h_k) from a probability distribution that is proportional to the approximation error $|r(z_i; \mathbf{w}^{(k-1)}) - H(z_i)|$, for $(z_i, H(z_i)) \in \mathbb{D}$ and $i = 1, 2, \dots, M$. A second alternative that we recommend is to change to a relative error measure, that is, we choose (λ_k, h_k) deterministically via

$$(\lambda_k, h_k) = \underset{(z_i, H(z_i)) \in \mathbb{D}, H(z_i) \neq 0}{\operatorname{argmax}} \frac{|r(z_i; \mathbf{w}^{(k-1)}) - H(z_i)|}{|H(z_i)|}. \quad (55)$$

We emphasize that we only use either of these two alternative greedy selection strategies if the weights $\mathbf{w}^{(k)}$ are chosen according to (53), i.e., the Levy approximation, **SK** iteration, and **WF** iteration all failed to decrease the rational approximation error. Only in this scenario, we replace [Algorithm 4](#) of [Algorithm 4](#) with either the probabilistic greedy step (54) or the relative error greedy step (55). While in general the performance of these alternatives to the classical greedy step depends on the problem, we have observed that in all considered examples either method is sufficient to prevent the stagnation of **NL-AAA**.

5 Numerical experiments

In this section, we demonstrate the performance of our proposed **NL-AAA** method in comparison to the classical **AAA** on both generic functions and reduced-order modeling benchmark problems. The experiments reported here were performed on a 2023 MacBook Pro

equipped with 16 GB RAM and an Apple M2 Pro chip. Computations were done in MATLAB 25.1.0.2973910 (R2025a) Update 1 running on macOS Sequoia 15.6.1. The source codes, data and results of the numerical experiments are available at [1].

5.1 Experimental setup

For each of the examples presented below, we have generated data sets of the form

$$\mathbb{D} = \{(z_1, H(z_1)), (z_2, H(z_2)), \dots, (z_M, H(z_M))\}, \quad (56)$$

where $H: \mathbb{C} \rightarrow \mathbb{C}$ denotes the original function that we aim to approximate.

For the comparison of the AAA and NL-AAA methods in terms of approximation quality, we compute and plot normalized versions of the discrete ℓ_2 and ℓ_∞ error measures over the respective data set \mathbb{D} given by

$$\frac{\left(\sum_{i=1}^M |H(z_i) - r(z_i)|^2 \right)^{1/2}}{\left(\sum_{i=1}^M |H(z_i)|^2 \right)^{1/2}} \quad \text{and} \quad \frac{\max_{(z, H(z)) \in \mathbb{D}} |H(z) - r(z)|}{\max_{(z, H(z)) \in \mathbb{D}} |H(z)|}. \quad (57)$$

For NL-AAA, in the steps in which the refinement strategies (SK and WF iterations) fail to decrease the approximation error, we are changing to the randomized greedy selection as outlined in Section 4.3. The supplemental code [1] also provides the option to change to the relative error measures as the alternative support point selection criterion.

5.2 Classical function approximations

As the first test of our proposed method, we aim to approximate two more generic nonlinear functions, namely $|\sin(3\pi x)|$ and triWave(x) (defined below), via rational functions similar to the motivating examples presented in Section 1. These two functions are chosen as they distill certain features, which lead to unsatisfactory convergence behavior of the classical AAA method. On the other hand, the proposed NL-AAA does not seem to be negatively affected by these features. Furthermore, these functions include sharp, non-differentiable edges that can be also seen in model order reduction benchmarks; see Section 5.3 for further details.

Let us first consider the approximation of $|\sin(3\pi x)|$ in the real interval $x \in [-1, 1]$. As data, we have sampled the function in 1000 real, linearly equidistant points in the considered interval and used this data to compute rational approximations via AAA and NL-AAA up to degree 50. The convergence of the two methods in the normalized (squared) ℓ_2 -norm is shown in Figure 3a. We can see that while the error of the AAA approximation tends downwards, it is far from monotonic and has large variations in the magnitude of the error that can be observed as spikes in the plot. In contrast, the NL-AAA approximation error monotonically decreases over the iterations and has smaller errors than AAA in nearly every step. For degree 50, both methods yield a suitable approximation to the given function $f(x) = |\sin(3\pi x)|$ as can be seen in Figure 3c.

In general, we have observed that AAA tends to struggle with its error convergence and approximation quality when the function underlying the given data is less smooth and has points at which the derivative changes rapidly or does not exist. Another function of that type is the triangular wave. This function is defined on the interval $x \in [-1, 1]$ via

$$\text{triWave}(x) = 2 \left| 3x - \left\lfloor 3x + \frac{1}{2} \right\rfloor \right|, \quad (58)$$

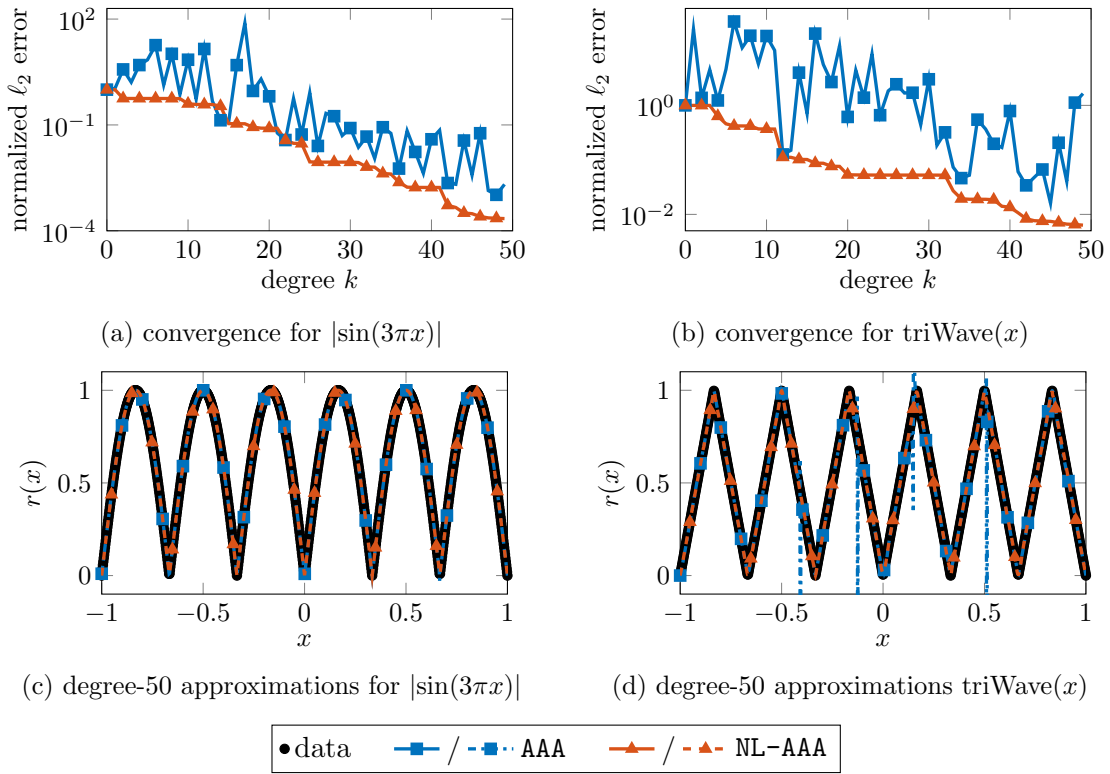


Figure 3: Convergence and approximation results of **AAA** and **NL-AAA** for the functions $|\sin(3\pi x)|$ and $\text{triWave}(x)$: For both example functions, the classical **AAA** has a very unsteady error convergence while the proposed **NL-AAA** provides a monotonic decay. For the triWave function, the final approximation by **AAA** shows visible deviations from the given data while **NL-AAA** provides an indistinguishable approximation.

where $\lfloor \cdot \rfloor$ denotes the integer floor function. In contrast to the previous function $|\sin(3\pi x)|$, the triangular wave has double the amount of non-differentiable points in the interval $[-1, 1]$. This particular triangular wave can also be obtained via the piecewise linear interpolation of $|\sin(3\pi x)|$.

As for the previous function, we sample $\text{triWave}(x)$ in 1 000 real, linearly equidistant points in the interval $[-1, 1]$ to construct our data, and then we use **AAA** and **NL-AAA** to construct rational approximations up to degree 50. In Figure 3b, we see that this time the errors of **AAA** and **NL-AAA** lie even further apart. As for the previous example, we see that the error behavior of **AAA** yields many rapid changes. However, this time no general convergence trend is visible and most of the approximations constructed via **AAA** up to degree 50 yield a normalized ℓ_2 error that is larger than 1. The degree-50 approximations in Figure 3d show that in several points, the **AAA** approximation strongly deviates from the given data. On the other hand, the proposed **NL-AAA** algorithm provides again a monotonic error decay and the degree-50 approximation is indistinguishable from the given data.

5.3 Model order reduction benchmark examples

The previous numerical examples have indicated that functions with sharp edges and non-differentiable points pose a larger challenge for the classical **AAA** algorithm compared to our proposed **NL-AAA** method. For many model order reduction examples, similar behaviors

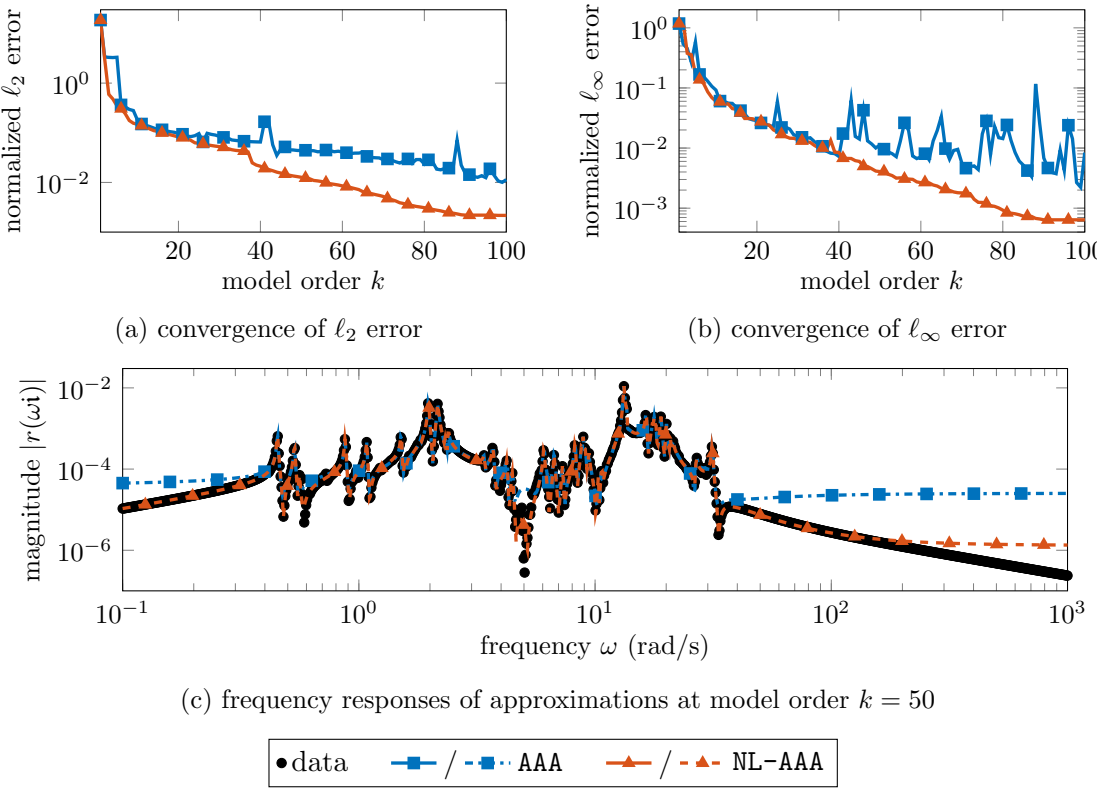


Figure 4: Convergence and approximation results of AAA and NL-AAA for the transfer function of the international space station model: The proposed NL-AAA provides a monotonic convergence in the ℓ_2 error but also convinces in the ℓ_∞ error. For larger model orders, the error of the classical AAA is visibly larger than for NL-AAA in both error metrics.

can be observed with data given close to non-differentiable points with quickly varying function values. In the following, we compare the AAA and NL-AAA algorithms on two established model order reduction examples from the literature. As we consider here the underlying dynamical systems rather than the corresponding rational functions, we denote the complexity of the results by the order of the underlying model, which is the degree of the corresponding rational transfer function plus one.

5.3.1 International space station

The first model order reduction example we consider is a dynamical system model of stage 12A of the international space station (ISS) [15, 23]. The transfer function corresponding to the dynamical system is a matrix-valued rational function of degree 1412. As we consider scalar functions in this work, we only take the upper left entries of these matrix-valued transfer functions. This models the input-to-output behavior of the system from the first system input to the first observed system output. To generate data for this example, we sample the transfer function at 1000 logarithmically equidistant points on the imaginary axis in the interval $[10^{-1}, 10^3]i$. This range captures the main behavior of the system's frequency response. The magnitudes of the sampled data points are shown in Figure 4c.

Convergence of AAA and NL-AAA in the normalized ℓ_2 norm is shown in Figure 4a. Due to its importance for the modeling of dynamical systems, we also show the corresponding convergence in the ℓ_∞ norm in Figure 4b. While initially as good as NL-AAA, the classical

AAA algorithm diverges in accuracy in both error metrics after model order $k = 40$. This discrepancy increases for the remainder of the model orders displayed until the final iteration $k = 100$, where the NL-AAA approximation has a normalized ℓ_2 error of 0.0014 while AAA provides an error of 0.0113. Thus, NL-AAA performs one order of magnitude better in terms of accuracy for the final approximation size. As discussed in [Section 4.3](#), we see that NL-AAA decreases the ℓ_2 error monotonically in [Figure 4a](#). While the same claim does not hold for the ℓ_∞ norm, we see in [Figure 4b](#) that the ℓ_∞ error of the NL-AAA approximation decreases monotonically nearly everywhere.

We emphasize that in model order reduction, the construction of highly accurate models of smallest order is critical. Furthermore, in many applications, a normalized ℓ_2 error of about 1% is considered as sufficiently accurate. The proposed NL-AAA achieves this target accuracy already at iteration $k = 56$, while AAA does not reach that accuracy even at iteration 100. In [Figure 4c](#), the frequency responses of the two approximations at model order $k = 50$ are shown together with the sampled data. We can see the qualitatively better fit provided by NL-AAA. While both approaches are able to accurately match the peaks in the data, the data in between these peaks is visibly better matched by NL-AAA.

5.3.2 Vibrating plate

As a second model order reduction example, we consider the vibrational response of a struttured plate from [5, 26]. This plate has been equipped with a set of tuned vibration absorbers, which dampen the response of the plate around the frequency 48 Hz. The vibrations are measured as root mean squared displacement of the internal area of the plate in the vertical direction. The data for this model are transfer function samples given at linearly equidistant points in the interval $[1, 250] \cdot 2\pi i$. Since the transfer function of this model is a real-valued function on the complete complex plane, it is not analytic in any open subset of the complex plane. We use the two algorithms, AAA and NL-AAA, to compute approximations to the sampled data up to model order 60.

The results of the computations can be seen in [Figure 5](#). The normalized errors in [Figures 5a](#) and [5b](#) show the differences in the convergence behavior between AAA and NL-AAA. As expected from the previous generic function examples, the classical AAA method struggles with the data coming from a function with several non-analytic points compared to the previous model reduction benchmark. This can be seen in [Figures 5a](#) and [5b](#) by the large error deviations between iterations in either error metric. In contrast, NL-AAA provides the guaranteed monotonic error behavior in the normalized ℓ_2 norm and a similarly smooth and reliable error convergence in the ℓ_∞ norm. We can also see that overall the error of NL-AAA is at least as good as AAA but significantly smaller for most approximation orders.

[Figure 5c](#) shows the frequency response of the approximations computed via AAA and NL-AAA for the model order $k = 50$ in comparison to the given data. For this example, we see that the larger error of the AAA approximation stems from localized inaccuracies close to the given data, e.g., at about $630i$, there is a large, visible spike in the AAA model that is not present in the original data. Similar to the examples in [Section 4.2.3](#), we have observed that the denominator of the AAA approximation largely varies up to five order of magnitude over the approximation range, which may explain the inaccuracies. In contrast, we can see in [Figure 5c](#) that the NL-AAA approximation accurately matches the given data.

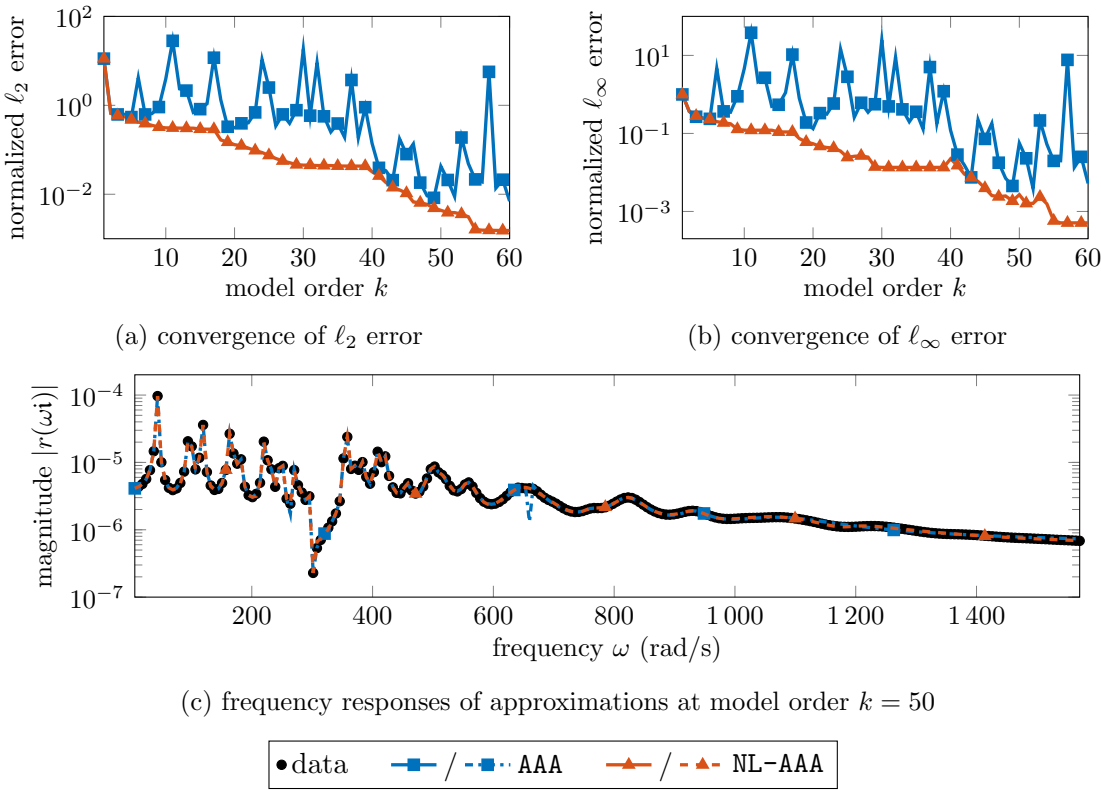


Figure 5: Convergence and approximation results of AAA and NL-AAA for the transfer function of the vibrating plate: The proposed NL-AAA method provides a smooth and reliable decaying error behavior in both considered error metrics, while the classical AAA has rapid changes in its approximation quality with an overall larger error. For model order 50, the frequency response shows that AAA introduces localized inaccuracies while NL-AAA fits the data without visible differences.

6 Conclusions

We introduced a new greedy approach for the construction of rational approximations for given data. Similar to the classical AAA algorithm, the proposed method greedily selects barycentric interpolation points based on an ℓ_∞ measure and subsequently fits the barycentric weights to approximate the remaining data. In contrast to the classical approach, we propose to use efficient refinement procedures to solve the true rational least-squares problem to fit the remaining data rather than fitting only a linearization. The design of our algorithm is supported by the theoretical analysis of the gradients used in the different minimization approaches, which provides a more reliable and monotonic error behavior compared to AAA. This has been practically verified via numerical experiments using classical problems from function approximation as well as model order reduction benchmarks.

Acknowledgments

The work of Ackermann was supported in part by the Simons Dissertation Fellowship in Mathematics. The works of Balicki and Gugercin were supported in part by US National Science Foundation grant DMS-2411141.

References

- [1] M. S. Ackermann, L. Balicki, and S. W. R. Werner. Code, data and results for numerical experiments in “A refined nonlinear least-squares method for the rational approximation problem” (version 1.0), January 2026. [doi:10.5281/zenodo.18317028](https://doi.org/10.5281/zenodo.18317028).
- [2] A. C. Antoulas. *Approximation of Large-Scale Dynamical Systems*, volume 6 of *Adv. Des. Control*. SIAM, Philadelphia, PA, 2005. [doi:10.1137/1.9780898718713](https://doi.org/10.1137/1.9780898718713).
- [3] A. C. Antoulas and B. D. O. Anderson. On the scalar rational interpolation problem. *IMA J. Math. Control Inf.*, 3(2–3):61–88, 1986. [doi:10.1093/imamci/3.2-3.61](https://doi.org/10.1093/imamci/3.2-3.61).
- [4] A. C. Antoulas, C. A. Beattie, and S. Gugercin. *Interpolatory Methods for Model Reduction*. Computational Science & Engineering. SIAM, Philadelphia, PA, 2020. [doi:10.1137/1.9781611976083](https://doi.org/10.1137/1.9781611976083).
- [5] Q. Aumann and S. W. R. Werner. Structured model order reduction for vibro-acoustic problems using interpolation and balancing methods. *J. Sound Vib.*, 543:117363, 2023. [doi:10.1016/j.jsv.2022.117363](https://doi.org/10.1016/j.jsv.2022.117363).
- [6] P. Benner, V. Mehrmann, and D. C. Sorensen. *Dimension Reduction of Large-Scale Systems*, volume 45 of *Lect. Notes Comput. Sci. Eng.* Springer, Berlin, Heidelberg, 2005. [doi:10.1007/3-540-27909-1](https://doi.org/10.1007/3-540-27909-1).
- [7] P. Benner, W. Schilders, S. Grivet-Talocia, A. Quarteroni, G. Rozza, and L. M. Silveira. *Model Order Reduction. Volume 1: System- and Data-Driven Methods and Algorithms*. De Gruyter, Berlin, Boston, 2021. [doi:10.1515/9783110498967](https://doi.org/10.1515/9783110498967).
- [8] M. Berljafa and S. Güttel. Generalized rational Krylov decompositions with an application to rational approximation. *SIAM J. Matrix Anal. Appl.*, 36(2):894–916, 2015. [doi:10.1137/140998081](https://doi.org/10.1137/140998081).
- [9] M. Berljafa and S. Güttel. The RKFIT algorithm for nonlinear rational approximation. *SIAM J. Sci. Comput.*, 39(5):A2049–A2071, 2017. [doi:10.1137/15M1025426](https://doi.org/10.1137/15M1025426).
- [10] J.-P. Berrut and L. N. Trefethen. Barycentric Lagrange interpolation. *SIAM Rev.*, 46(3):501–517, 2004. [doi:10.1137/S0036144502417715](https://doi.org/10.1137/S0036144502417715).
- [11] D. Deschrijver, T. Dhaene, and G. Antonini. A convergence analysis of iterative macromodeling methods using Whitfield’s estimator. In *2006 IEEE Workshop on Signal Propagation on Interconnects*, pages 197–200, 2006. [doi:10.1109/SPI.2006.289219](https://doi.org/10.1109/SPI.2006.289219).
- [12] S. Dirckx, K. Meerbergen, and D. Huybrechs. QR-based parallel set-valued approximation with rational functions. e-print 2312.10260, arXiv, 2023. Numerical Analysis (math.NA). [doi:10.48550/arXiv.2312.10260](https://doi.org/10.48550/arXiv.2312.10260).
- [13] Z. Drmač, S. Gugercin, and C. Beattie. Quadrature-based vector fitting for discretized \mathcal{H}_2 approximation. *SIAM J. Sci. Comput.*, 37(2):A625–A652, 2015. [doi:10.1137/140961511](https://doi.org/10.1137/140961511).
- [14] I. V. Gosea, S. Gugercin, and C. Beattie. Data-driven balancing of linear dynamical systems. *SIAM J. Sci. Comput.*, 44(1):A554–A582, 2022. [doi:10.1137/21M1411081](https://doi.org/10.1137/21M1411081).

- [15] S. Gugercin, A. C. Antoulas, and M. Bedrossian. Approximation of the international space station 1R and 12A models. In *Proceedings of the 40th IEEE Conference on Decision and Control*, pages 1515–1516, 2001. [doi:10.1109/CDC.2001.981109](https://doi.org/10.1109/CDC.2001.981109).
- [16] B. Gustavsen and A. Semlyen. Rational approximation of frequency domain responses by vector fitting. *IEEE Trans. Power Del.*, 14(3):1052–1061, 1999. [doi:10.1109/61.772353](https://doi.org/10.1109/61.772353).
- [17] J. M. Hokanson. Multivariate rational approximation using a stabilized Sanathanan-Koerner iteration. e-print 2009.10803, arXiv, 2020. Numerical Analysis (math.NA). [doi:10.48550/arXiv.2009.10803](https://doi.org/10.48550/arXiv.2009.10803).
- [18] A. C. Ionita. *Lagrange rational interpolation and its applications to approximation of large-scale dynamical systems*. Dissertation, Rice University, Houston, Texas, USA, 2013. URL: <https://hdl.handle.net/1911/77180>.
- [19] K. Kreutz-Delgado. The complex gradient operator and the CR-calculus. e-print 0906.4835, arXiv, 2009. Optimization and Control (math.OC). [doi:10.48550/arXiv.0906.4835](https://doi.org/10.48550/arXiv.0906.4835).
- [20] E. C. Levy. Complex-curve fitting. *IRE Trans. Autom. Control*, AC-4(1):37–43, 1959. [doi:10.1109/TAC.1959.6429401](https://doi.org/10.1109/TAC.1959.6429401).
- [21] A. Ma and A. Ege Engin. Orthogonal rational approximation of transfer functions for high-frequency circuits. *Int. J. Circuit Theory Appl.*, 51(3):1007–1019, 2022. [doi:10.1002/cta.3488](https://doi.org/10.1002/cta.3488).
- [22] A. J. Mayo and A. C. Antoulas. A framework for the solution of the generalized realization problem. *Linear Algebra Appl.*, 425(2–3):634–662, 2007. Special issue in honor of P. A. Fuhrmann, Edited by A. C. Antoulas, U. Helmke, J. Rosenthal, V. Vinnikov, and E. Zerz. [doi:10.1016/j.laa.2007.03.008](https://doi.org/10.1016/j.laa.2007.03.008).
- [23] MORwiki Benchmark Collection. Iss-12a. hosted at MORwiki – Model Order Reduction Wiki. URL: https://modelreduction.org/morwiki/International_Space_Station.
- [24] Y. Nakatsukasa, O. Sète, and L. N. Trefethen. The AAA algorithm for rational approximation. *SIAM J. Sci. Comput.*, 40(3):A1494–A1522, 2018. [doi:10.1137/16M1106122](https://doi.org/10.1137/16M1106122).
- [25] Y. Nakatsukasa and L. N. Trefethen. Applications of AAA rational approximation. e-print 2510.16237, arXiv, 2025. Numerical Analysis (math.NA). [doi:10.48550/arXiv.2510.16237](https://doi.org/10.48550/arXiv.2510.16237).
- [26] S. Reiter and S. W. R. Werner. Interpolatory model reduction of dynamical systems with root mean squared error. *IFAC-Pap.*, 59(1):385–390, 2025. 11th Vienna International Conference on Mathematical Modelling MATHMOD 2025. [doi:10.1016/j.ifacol.2025.03.066](https://doi.org/10.1016/j.ifacol.2025.03.066).
- [27] C. Sanathanan and J. Koerner. Transfer function synthesis as a ratio of two complex polynomials. *IEEE Trans. Autom. Control*, 8(1):56–58, 1963. [doi:10.1109/TAC.1963.1105517](https://doi.org/10.1109/TAC.1963.1105517).
- [28] A. H. Whitfield. Asymptotic behaviour of transfer function synthesis methods. *Int. J. Control.*, 45(3):1083–1092, 1987. [doi:10.1080/00207178708933791](https://doi.org/10.1080/00207178708933791).

[29] W. Wirtinger. Zur formalen Theorie der Funktionen von mehr komplexen Veränderlichen. *Math. Ann.*, 97(1):357–375, 1927. [doi:10.1007/BF01447872](https://doi.org/10.1007/BF01447872).